

Oxygen isotope variations in rainfall, drip-water and speleothem calcite from a well-ventilated cave in Texas, USA: Assessing a new speleothem temperature proxy

Weimin Feng^{a,*}, Richard C. Casteel^a, Jay L. Banner^a, Ayla Heinze-Fry^{a,b}

^a Jackson School of Geosciences, The University of Texas at Austin, Austin, TX, United States

^b Department of Geological Sciences, The University of Massachusetts, Amherst, MA, United States

Received 9 May 2013; accepted in revised form 26 November 2013; available online 7 December 2013

Abstract

Measurements of the oxygen isotopic composition ($\delta^{18}\text{O}$ value) of rainfall, drip-water and associated calcite (grown on artificial substrates and in a natural speleothem) at multiple drip sites in a well-ventilated cave in central Texas were conducted to investigate the potential use of speleothem $\delta^{18}\text{O}$ for quantitative temperature reconstructions. From 2009 to 2011, rainfall $\delta^{18}\text{O}$ varied by 11.5‰ (−10.5‰ to 1.0‰, V-SMOW), whereas drip-waters had a much narrower range of 0.3‰ (−4.7‰ to −4.4‰, V-SMOW). This contrast indicates that mixing processes along flow paths in the vadose zone above the cave produce a well-homogenized water reservoir that supplies drip-water to the cave. The $\delta^{18}\text{O}$ values for calcite grown on substrates over the same time period show seasonal variations (summer: \sim −6‰; winter: \sim −3‰) that are strongly correlated with surface air temperatures (t_a) at all three monitored sites ($r^2 = 0.88$ – 0.96 ; $p < 0.001$). These results indicate that the dominant control on calcite $\delta^{18}\text{O}$ is temperature. An empirical relationship was established for one monitored site: $t_a = -9.1 (\pm 0.9) \times \delta^{18}\text{O} \times 10^3 - 20.6 (\pm 4.1)$; $r^2 = 0.88$, and applied to a $\delta^{18}\text{O}$ time series of the top 6.7 mm of a stalagmite that grew at this drip site. This yields a temperature record that appears to reflect seasonal variations for the period 2005–2009. This speleothem-derived temperature record is offset to lower values (by 0–8 °C) compared to the instrumental temperature record. This offset may be a result of differences between substrate and speleothem calcite in terms growth mechanism, extent of non-equilibrium isotopic effects, or temporal shifts in drip-water $\delta^{18}\text{O}$ values. Despite this offset, the speleothem-derived record reconstructs the amplitudes of seasonal variations and changes in inter-annual summer peak temperatures in the instrumental record. Results of this study have implications for reconstructing past temperatures, and for establishing a speleothem chronology with seasonal resolution, using speleothem calcite $\delta^{18}\text{O}$. The results also suggest that relatively seldom-studied speleothem samples near the entrances of caves, where environmental conditions may be similar to surface conditions, could prove valuable as paleo-temperature archives.

© 2013 Elsevier Ltd. All rights reserved.

1. INTRODUCTION

Oxygen isotope ($\delta^{18}\text{O}$) studies of Pleistocene and Holocene speleothems often interpret these records in terms of variations in rainfall amount, air temperature and moisture source on decadal to millennial time scales (Bar-Matthews

et al., 1999; Hu et al., 2008; Matthey et al., 2008; Wagner et al., 2010). The interpretation of paleotemperature information from speleothems, however, may be complicated by the simultaneous effects on $\delta^{18}\text{O}$ of rainfall amount, temperature and moisture source, and by the potential for non-equilibrium (or ‘kinetic’) isotope effects during speleothem formation (Hendy, 1971; Mickler et al., 2004, 2006; Feng et al., 2012). These influences on speleothem $\delta^{18}\text{O}$ values may be expressed regionally, such as (1) the intensity of ENSO (e.g., Lachniet et al., 2004); (2) frequency of tropical cyclones (Frappier et al., 2007); (3) the strength of the Asian

* Corresponding author. Current address: Department of Physics, Astronomy and Geosciences, Valdosta State University, Valdosta, GA, United States. Tel.: +1 2147147264.

E-mail address: weimin.feng@gmail.com (W. Feng).

and North American Monsoon (e.g., Wang et al., 2001; Cheng et al., 2009); (4) the position and strength of the polar jet stream (e.g., Asmerom et al., 2010); and (5) the position of the Intertropical Convergence Zone (e.g., Shakun et al., 2007).

Temperature affects speleothem $\delta^{18}\text{O}$ values through two different processes: (1) the global distribution of rainfall $\delta^{18}\text{O}$ values is correlated with temperature in mid- to high-latitude regions (Rozanski et al., 1993) due to the temperature dependence of both rainfall amount and the liquid–vapor fractionation factor for oxygen isotopes; (2) calcite deposited from solution will acquire varying degrees of enrichment of ^{18}O in the mineral according to temperature-dependent equilibrium fractionation factor (Epstein et al., 1953; Friedman and O’Neil, 1977; Kim and O’Neil, 1997; Coplen, 2007). In ideal cases, the effects of the combination of these two processes may be used to infer changes in past temperatures from speleothem $\delta^{18}\text{O}$ values. However, because rainfall $\delta^{18}\text{O}$ is affected by other factors (e.g., moisture source, rainfall amount), such inferences regarding past temperatures commonly have significant uncertainties. In the central Texas cave of the present study, drip-waters have a very limited range of $\delta^{18}\text{O}$ values over multi-year period. This limited variability renders the influence of temperature on rainfall $\delta^{18}\text{O}$ (process 1 above) and other surface processes negligible, which in turn constrains the influence of temperature to occur via in-cave processes such as calcite-water fractionation (process 2). Other in-cave processes affecting speleothem calcite $\delta^{18}\text{O}$ values include kinetic isotopic fractionation (e.g., Hendy, 1971; Mickler et al., 2004, 2006; Feng et al., 2012); water evaporation, whereby enhanced evaporation increases $\delta^{18}\text{O}$ values of both drip-water and calcite (e.g., Hendy, 1971; Deininger et al., 2012); and changes in drip rate, whereby higher drip rates replenish the water film on the speleothem surface faster and negate the impact of evaporation (e.g., Scholz et al., 2009).

Most speleothem studies have focused on samples forming deep in the cave environment, where meteorological conditions such as relative humidity, cave-air CO_2 concentrations, and evaporation rates are stable compared to the cave exterior. These speleothems, however, tend to grow relatively slowly due to high cave-air CO_2 concentrations (e.g., Banner et al., 2007) and are subject to little to no seasonal temperature variability. Sub-annual $\delta^{18}\text{O}$ variations that are occasionally found in speleothems from these deep settings are likely influenced by factors other than or in addition to temperature (e.g., Johnson et al., 2006; Matthey et al., 2008). Recent advances in extracting temperature related information from speleothems include application of clumped isotopes and isotopic and noble gas analysis of fluid inclusions (Affek et al., 2008; Kluge et al., 2008; Scheidegger et al., 2010). The clumped isotope methodology demonstrates significant potential for obtaining absolute temperatures from analysis of carbonate minerals. Applications to speleothems, however, indicate that calcite growth in cave environments is often fraught with significant kinetic effects on clumped-isotope variations (Affek et al., 2008; Daëron et al., 2011), which limits the extraction of temperature information from speleothems. Fluid inclusion

studies, in practice, require a significant amount of sample (>0.5 g, e.g., Vonhof et al., 2006), which limits its use in high-resolution climate reconstruction using speleothems. The $\delta^{18}\text{O}$ records of speleothems from well-constrained environments, therefore, may present an important opportunity for the construction of high-resolution paleotemperature records.

The present study aims to advance temperature reconstruction from speleothem $\delta^{18}\text{O}$ records by evaluating the relationship between temperature and $\delta^{18}\text{O}$ values of drip-water and speleothem calcite. We studied a shallow cave environment in central Texas characterized by large seasonal temperature shifts. We present $\delta^{18}\text{O}$ results for rainfall, drip-water, calcite formed on artificial substrates placed under active drips, and calcite sampled from an actively growing stalagmite. These results are then compared with meteorological conditions over the same time period to evaluate the relationship between speleothem $\delta^{18}\text{O}$ values and surface air temperatures.

2. HYDROGEOLOGIC SETTING

Westcave Preserve (Fig. 1a) is located within the Heinz Branch watershed in central Texas, on the eastern edge of the Edwards Plateau (Fig. 1b). The study site is a small, shallow cave in the Preserve. The regional climate ranges from subtropical/sub-humid to semi-arid (Larkin and Bomar, 1983). In terms of temperature and rainfall, this amounts to dry, hot summers, generally wetter springs and falls, and dry, mild winters. The probability for drought in the region is high with intermittent droughts dispersed amongst wetter periods (Banner et al., 2010). For the study period from July 2009 to February 2011, mean annual rainfall was ~ 91 cm (measured at the Preserve), while mean monthly temperature (MMT) ranged from 8 to 32 °C (NOAA station ID: GHCND: US1TXTV0019). The region experienced a record drought and high temperatures (MMT > 33 °C) in the summer of 2011 (Combs, 2012).

Thin soils (<20 cm) in the region support pasture grasses, Ashe juniper trees and shrubs, and oaks, on a substrate of the Lower Cretaceous Cow Creek Limestone Formation. The cave (“Westcave” hereafter) formed along the wall of a 30-m-deep canyon by travertine draping over and partly enclosing an overhang of resistant Cow Creek strata (Caran, pers. comm., 2012). The overburden above the drip sites is ~ 20 – 25 m thick. The cave has a volume of ~ 1400 m³ (LHW $\sim 35 \times 5 \times 8$ m) and several openings (Fig. 1a), resulting in an opening area to cave volume ratio of ~ 0.02 m⁻¹. This large ratio and multiple openings allow the cave to ventilate throughout the year. This is in contrast to other caves in the region that are deeper, have much smaller opening area to cave volume ratios (~ 0.001 – 0.0003 m⁻¹), and ventilate seasonally (Banner et al., 2007; Feng et al., 2012; Cowan et al., 2013). As a result, Westcave has an internal atmosphere with temperature and CO_2 concentrations similar to that of the surface atmosphere (Casteel, 2011). The narrow range and low, near atmospheric, values of cave-air CO_2 concentrations (volume fraction: 420–640 ppm; Fig. 2) throughout the year allow for year-round calcite growth, in contrast to the strong

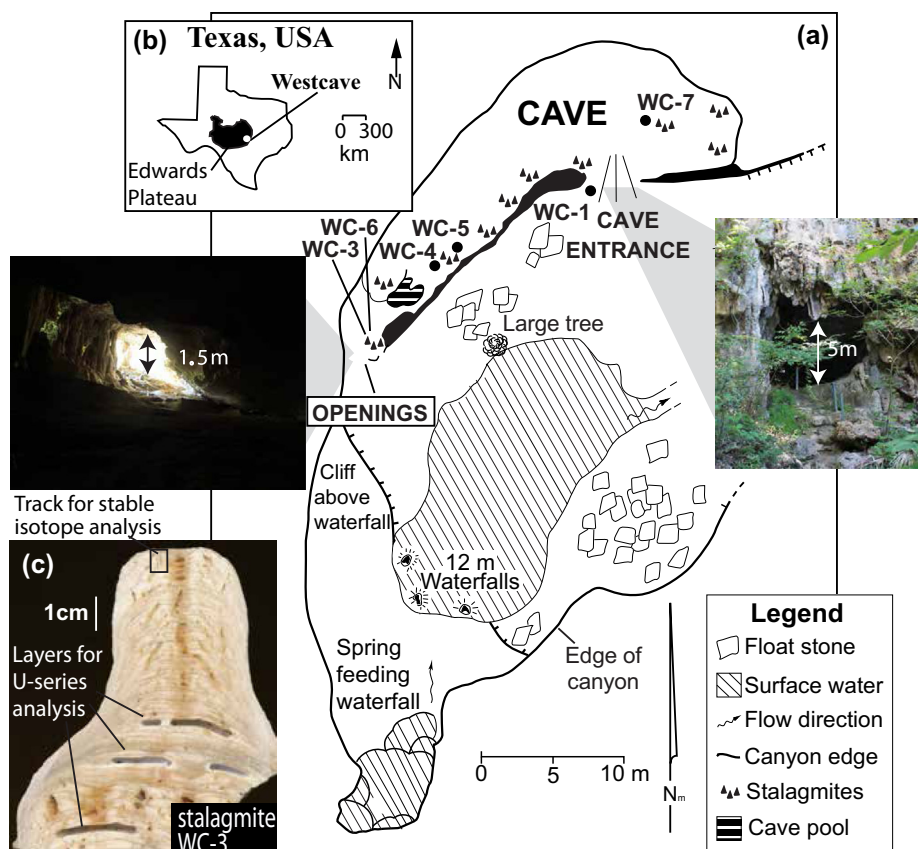


Fig. 1. Location map and cave map for Westcave Preserve. (a) Map of Westcave; monitored sites are labeled; (b) location of Westcave Preserve in Texas, USA; (c) image of stalagmite WC-3. Top 6.7 mm (area indicated by a box) are micromilled at 167 μm steps for stable isotope analysis. Three layers sampled at depths of 5.0, 6.5 and 8.0 cm for U-series dating are also marked (Table 7).

seasonality in cave-air CO_2 and calcite growth observed in other caves in the region (Banner et al., 2007; Feng et al., 2012; Cowan et al., 2013). A $\sim 200 \text{ m}^2$ pond fed by a waterfall sits near the cave openings, which may help maintain elevated relative humidity in the cave and moderate local temperature (Fig. 1a).

An ongoing monitoring study at Westcave has provided samples and measurements of environmental parameters since July 2009 (Casteel and Banner, 2011). The present study presents results from three drip sites (WC-1, 3, 6; Fig. 1a). For WC-1 and WC-3, drips emanate from soda straws (2.5–15 cm in length), while the drip for WC-6 flows down a 30-cm-long drapery prior to drip. The drip rates for these sites are not influenced by rainfall variations and are thus considered to be fed by diffuse flow paths (Casteel and Banner, 2011).

3. METHODS AND SAMPLES

3.1. Sample collection

Methods of cave monitoring and sample collection follow protocols developed over a 12-yr period (e.g., Musgrove and Banner, 2004; Banner et al., 2007; Feng

et al., 2012; Cowan et al., 2013). Relevant methods are briefly described below.

Sampling was conducted every 4–5 weeks at Westcave since July 2009. Monitored cave conditions include cave-air CO_2 concentration, cave-air temperature (t_c), relative humidity (RH), drip rate, and drip-water temperature (t_w). Collection time for water samples ranged from 40 min to 4–6 h, depending on the drip rate. Drip-water temperatures were measured after water sample collection. To determine if drip-water temperature changes from the discharge point on the cave ceiling to the collection in the bottle, direct measurements of water temperature from drapery and stalactite tips were also carried out for collection trips from January 2011 to June 2013. The results were compared to the measurements made on water collected in the bottles during the same field trips. This test showed no significant differences (on average $<1^\circ\text{C}$) between the two methods of measurement, indicating that before dripping, drip-water attains a stable temperature, which it likely maintains during speleothem calcite deposition. Upon collection, aliquots of drip-water for oxygen isotope analysis were transferred to clean 4-ml glass vials. Vials are filled and sealed with screw thread cap with Polytetrafluoroethylene/Silicone septa, wrapped with Parafilm, and kept refrigerated until analysis.

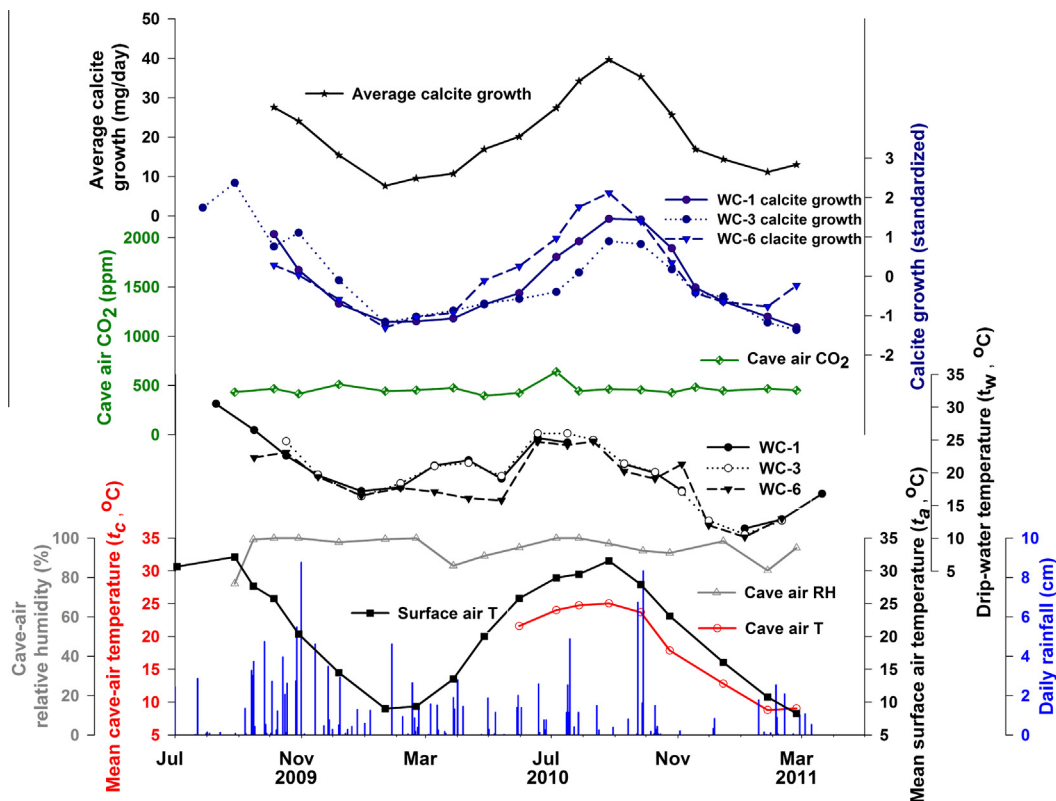


Fig. 2. Time series of daily rainfall, mean monthly surface air temperature (t_a), cave-air temperature (t_c), cave-air relative humidity (RH), cave-air CO_2 concentration, drip-water temperature (t_w) and calcite growth for three drip sites, and average calcite growth for all sites. Calcite growth rates for each site are standardized to each drip site's mean growth rate. For each site, there is a positive correlation between calcite growth and t_a , t_c and t_w . Changes in cave-air CO_2 concentration are very small and do not correlate with calcite growth.

Sanded and cleaned 10×10 cm glass substrates were placed under monitored drip sites to collect calcite deposited from drip-water between consecutive field trips. Collected substrates were rinsed with deionized water on site and dried overnight in a laminar flow hood. Substrates were weighed using a Sartorius MC1 RC 210P electronic balance prior to deployment and after collection to calculate calcite growth (in units of mg/day, following methods in Banner et al., 2007).

An actively growing stalagmite WC-3 (underneath drip site WC-3, Fig. 1a) was sampled in July 2009, at the start of the monitoring study described above. The stalagmite is ~ 10 cm in length, comprised of white to pale orange growth bands of calcite, and has pores along its growth axis (Fig. 1c). The upper 6.7 mm of the stalagmite was sampled at an increment of $167 \mu\text{m}$ parallel to the growth axis using an automated micromill system. Of 40 milled samples, 37 had sufficient calcite for oxygen isotope analysis.

Daily rain gauge amounts are recorded by Westcave Preserve staff, and thus daily rainfall statistics were available for the study period. Daily surface air temperature (t_a) was obtained from the nearest weather station, located 11 km southeast of Westcave (Bee Cave, Texas; NOAA station ID: GHCND: US1TXTV0019). For isotopic analysis, rainfall samples were collected monthly from the roof of the Jackson Geological Sciences Building on the University of Texas at Austin campus, ~ 50 km to the east of Westcave.

3.2. Isotope analyses

Isotopic compositions ($\delta^{18}\text{O}$, $\delta^{13}\text{C}$ and δD values) were measured at the University of Texas at Austin. For water samples, $\delta^{18}\text{O}$ values were measured on CO_2 equilibrated with the water samples on a Thermo GasBench II connected to a Thermo ConFlo IV and a Thermo Delta V Plus. The δD values were measured on H_2 equilibrated with water. For the calcite samples, $\sim 200 \mu\text{g}$ of calcite powder were scraped with dental-grade steel tools and spatulas from an area close to the center of calcite growth when discernible or closest to the center of the substrate when there was no visible growth center. The $\delta^{18}\text{O}$ and $\delta^{13}\text{C}$ values were measured for CO_2 liberated from the mineral by reaction with H_3PO_4 in a Thermo Kiel IV Carbonate Device attached to a dual inlet Thermo MAT 253. Ten NBS 19 standards run with the unknown calcite samples yield a mean value of $2.20 \pm 0.10\text{‰}$ (2σ) (V-PDB) for $\delta^{18}\text{O}$. Oxygen isotopic results were reported relative to V-PDB standard (Craig, 1957). Conversions to V-SMOW/SLAP standard (Gonfiantini, 1978) were made using the following equation (Friedman and O'Neil, 1977):

$$\delta_{\text{V-SMOW}} = 1.03091\delta_{\text{V-PDB}} + 30.91 \quad (1)$$

Results are expressed on the normalized scale such that $\delta^{18}\text{O}$ of SLAP is -55.5‰ (Coplen, 1996). The δ notation is defined as:

$$\delta = R_{\text{sample}}/R_{\text{standard}} - 1 \quad (2)$$

For $\delta^{18}\text{O}$, R_{sample} and R_{standard} are the number ratios of $^{18}\text{O}/^{16}\text{O}$ in the sample and standard respectively.

3.3. U-series geochronology

Three growth layers of stalagmite WC-3 were analyzed using U-series methods (Fig. 1c) at the University of Texas at Austin. For each layer, after removal of the surface of the polished slab (~200 μm deep), ~500 mg calcite powder was hand-drilled in a laminar flow hood along the growth layer. Powdered samples were chemically prepared in a clean lab following the procedures of Musgrove et al. (2001), and measured for the U and Th isotope ratios on a Thermo-Fisher Triton thermal ionization mass spectrometer. Ages were calculated using published half-lives (Cheng et al., 2000), and were corrected for detrital thorium using an initial $^{230}\text{Th}/^{232}\text{Th}$ ratio of 5.8 ± 0.6 ppm measured at this drip site (calcite deposited in Westcave displays a large $^{230}\text{Th}/^{232}\text{Th}$ range of 5.8–15.2 ppm, Wortham et al., 2013).

4. RESULTS

4.1. Cave meteorological conditions and substrate calcite growth

Seasonal cycles are observed in mean monthly surface air temperature (t_a , 8–32 °C, Table 1), cave-air temperature (t_c , 9–25 °C, Table 1), and drip-water temperature (t_w , 10–27 °C, Table 2; Fig. 2) at Westcave. Note that t_w were measured every 4–5 weeks, rather than daily as t_a records. The three temperature records directly correlate with each

other, with peak values in July–October and the lowest values in December–February (Fig. 2). These large seasonal temperature ranges contrast with much narrower cave-air and drip-water temperature ranges (<5 °C) typical of most caves in the region (Banner et al., 2007; Feng et al., 2012; Cowan et al., 2013).

Monthly measurements of relative humidity in the cave ranged from 77% to 100% with an average of 95% (Table 1). Drip rates ranged from 1.6 to 8.0 $\mu\text{l/s}$ (WC-1), 0.02 to 2.2 $\mu\text{l/s}$ (WC-3), and 38 to 97 $\mu\text{l/s}$ (WC-6). There is no seasonal or other temporal pattern in the changes of drip rates (Table 2).

Cave-air CO_2 concentrations ranged from 390 to 640 ppm ($n = 18$, Table 1, Fig. 2), with a mean value of 460 ppm. These CO_2 values are near-atmospheric and at the low end of the 370–38,000 ppm range observed in most other caves monitored in central Texas (Banner et al., 2007; Feng et al., 2012; Cowan et al., 2013). In the absence of high cave-air CO_2 concentrations that inhibit calcite deposition (Banner et al., 2007), calcite growth on substrates at all monitored Westcave sites occurred year-round. Substrate growth rates ranged seasonally from 5 to 67 mg/day, with highest rates in summers (Table 2, Fig. 2). For WC-1, growth rates were 21–32 mg/day in the summer months and 7–9 mg/day in the winter months. For WC-3, growth rates were 11–28 mg/day in the summer months and 5–11 mg/day in the winter months. For WC-6, growth rates were 31–67 mg/day in the summer months and 11–19 mg/day in the winter months. A positive correlation between drip rate and calcite growth rate was observed for WC-6 ($r^2 = 0.43$) but not for WC-1 and WC-3. The fastest drip site (WC-6) had the highest mean calcite growth rate, while slowest drip site (WC-3) had the lowest mean growth rate.

Table 1
Meteorological conditions and substrate calcite growth rates at the Westcave.

Date	Avg. monthly t_a (°C) ^a	Avg. monthly t_c (°C)	RH (%) ^d	CO_2 (ppm) ^b	Ave. calcite growth for 3 sites (mg/day) ^c
8/28/2009	32.2		76.8	430	
9/15/2009	27.8		99.2	470	
10/5/2009	24.3		99.9	420	27.5
10/29/2009	20.4		99.9	510	24.0
11/18/2009	14.8				15.4
12/7/2009	8.9		97.8	440	7.6
1/21/2010	9.4		99.4	450	9.5
2/20/2010	13.5		99.9	480	10.7
3/28/2010	20.0		85.9	390	16.9
4/27/2010	25.5		90.9	420	20.1
5/31/2010	29.0	21.6	95.1	640	27.4
7/6/2010	29.6	24.0	99.9	440	34.2
7/28/2010	31.6	24.7	97.1	460	39.6
8/26/2010	28.2	25.0	97.1	450	35.3
9/28/2010	22.4	23.7	93.5	430	25.6
10/24/2010	18.1	17.9	92.4	480	16.9
12/15/2010	14.4	12.8	98.4	450	14.3
1/27/2011	10.4	8.8	83.5	470	11.1
2/24/2011	8.3	9.0	95.0	450	13.0

^a Surface air temperatures are from a weather station 11 km from Westcave, in Bee Cave, Texas (NOAA station ID: GHCND: US1TXTV0019).

^b Values are in volume fraction.

^c Deposited on a 10 × 10 cm glass substrate.

^d Measured at site WC-3.

Table 2

Substrate calcite growth conditions and drip-water and calcite oxygen isotope results.

Dates	Growth rate (mg/d)	Drip rate ($\mu\text{l/s}$)	t_w ($^{\circ}\text{C}$) ^a	$\delta^{18}\text{O}_{\text{cc}/\text{o}}$ ‰ V-PDB	$\delta^{18}\text{O}_{\text{w}/\text{o}}$ ‰ V-SMOW	α	$\Delta^{18}\text{O}_{\text{cc-e}/\text{o}}$ ‰ ^b
<i>WC-1</i>							
8/10/2009					−4.4		
9/16/2009	28.8	2.5	26.5	−5.7	−4.5	1.0297	−0.2
10/17/2009	20.5	7.4	22.6	−5.7	−4.6	1.0298	−0.9
11/17/2009	12.7	7.9	19.6	−4.7	−4.6	1.0308	−0.5
12/29/2009	8.4	5.5	17.2	−3.8	−4.6	1.0317	−0.1
2/5/2010	8.5	3.8	17.8	−3.8	−4.6	1.0317	0.0
3/10/2010	9.2	1.8	21.1	−4.2	−4.6	1.0313	0.3
4/12/2010	12.5	1.6	21.9	−5.0	−4.5	1.0304	−0.4
5/14/2010	15.1	1.6	19.1	−5.7	−4.5	1.0297	−1.7
6/18/2010	23.5	4.2	25.3	−6.2	−4.5	1.0291	−1.0
7/17/2010	27.2	4.2	24.6	−6.5	−4.5	1.0288	−1.4
8/11/2010	32.4	8.0		−6.6	−4.6	1.0288	
9/10/2010	32.2	7.4	21.3	−6.4	−4.7	1.0291	−1.8
10/10/2010	25.6	6.9	20.0	−5.3	−4.6	1.0302	−1.0
11/5/2010	16.4	7.0	17.3	−4.8	−4.5	1.0306	−1.2
12/1/2010	13.2	4.5		−4.8	−4.5	1.0306	
1/5/2011	9.6	4.5	11.5	−3.6	−4.5	1.0318	−1.2
2/10/2011	7.1	4.3	12.9		−4.4		
3/21/2011		5.0	16.8		−4.4		
<i>WC-3</i>							
7/16/2009	24.2			−5.6	−4.5	1.0298	
8/12/2009	28.1	0.02		−5.3	−4.5	1.0301	
9/16/2009	18.2	0.9		−5.2	−4.5	1.0302	
10/17/2009	20.3		24.8	−5.2	−4.5	1.0302	−0.1
11/17/2009	13	1.1	19.7	−4.0	−4.5	1.0314	0.1
12/29/2009	6.4	0.9	16.4	−3.3	−4.5	1.0322	0.2
2/5/2010	7.3	1.1	18.4		−4.5		
3/10/2010	8.3	1.1	21.0	−3.7	−4.5	1.0317	0.7
4/12/2010	9.4	1.0	21.5	−4.5	−4.5	1.0309	0.0
5/14/2010	10.1	1.0	19.5	−5.1	−4.5	1.0303	−1.0
6/18/2010	11.2	1.0	26.0	−5.5	−4.5	1.0299	−0.1
7/17/2010	14.2	1.0	26.0	−5.3	−4.5	1.0301	0.1
8/11/2010	19.0	1.0	25.0	−5.2	−4.5	1.0302	0.0
9/10/2010	18.6	1.1	21.4	−5.6	−4.5	1.0298	−1.1
10/10/2010	14.7	1.2	20.1	−4.7	−4.6	1.0308	−0.4
11/5/2010	11.0	2.0	17.1	−4.6	−4.6	1.0309	−0.9
12/1/2010	10.5	2.2	12.7	−3.9	−4.5	1.0315	−1.2
1/5/2011	6.4	2.2	10.6	−3.1	−4.5	1.0324	−0.9
2/10/2011	5.3	1.7	12.7	−3.8	−4.5	1.0316	−1.1
3/21/2011					−4.5		
5/11/2011					−4.9		
7/6/2011					−6.0		
8/18/2011					−5.7		
<i>WC-6</i>							
9/16/2009	35.6	38	22.3	−5.3			
10/17/2009	31.2	80.9	23.1	−5.3	−4.5	1.0301	−0.5
11/17/2009	20.5	71.3	19.4	−4.2	−4.5	1.0312	−0.1
12/29/2009	10.5	45.5	16.5	−3.3	−4.5	1.0322	0.2
2/5/2010		63.5	17.7	−3.4	−4.6	1.0322	0.4
3/10/2010	14.5	78.0	17.1	−3.9	−4.7	1.0317	−0.1
4/12/2010	28.8	76.4	16.1	−4.8	−4.7	1.0308	−1.2
5/14/2010	35.1	75.8	15.8	−5.3	−4.6	1.0302	−1.9
6/18/2010	47.4	97.0	24.7	−5.8	−4.5	1.0296	−0.7
7/17/2010	61.2	97.0	24.2	−5.6	−4.5	1.0298	−0.6
8/11/2010	67.4	89.0	24.8	−6.2	−4.5	1.0291	−1.1
9/10/2010	55.0	89.6	20.2	−6.1	−4.6	1.0294	−1.8
10/10/2010	36.6	90.0	19.1	−5.0	−4.6	1.0305	−0.9
11/5/2010	23.2	48.0	21.3	−4.5	−4.6	1.0310	0.0

(continued on next page)

Table 2 (continued)

Dates	Growth rate (mg/d)	Drip rate ($\mu\text{l/s}$)	t_w ($^{\circ}\text{C}$) ^a	$\delta^{18}\text{O}_{\text{cc}/\text{oo}}$ V-PDB	$\delta^{18}\text{O}_{\text{w}/\text{oo}}$ V-SMOW	α	$\Delta^{18}\text{O}_{\text{cc-e}/\text{oo}}$ ^b
12/1/2010	19.4	62.0	12.0	−4.1	−4.5	1.0313	−1.6
1/5/2011	17.3	62.0	10.2	−3.5	−4.5	1.0319	−1.4
2/10/2011	11.2	64.0	13.0		−4.4		

^a Values are either averaged over two field measurements during two consecutive field trips (when both values available), or a single measurement during a field trip carried out 20 days before or after the date specified.

^b Calculated using Eq. 4 and fractionation factor of Coplen (2007).

Table 3

Amount and isotopic compositions of Austin rainfall.^a

Date	$\delta^{18}\text{O}$ (V-SMOW, ‰)	δD (V-SMOW, ‰)	Austin rainfall amount (cm) ^b
4/27/2009	−2.5	−12	6.9
5/27/2009	−3.2	−16	4.7
6/27/2009	−2.3	−15	2.5
7/23/2009	1.0	8	0.2
8/22/2009	−2.2	−15	0.2
8/31/2009	−1.5		1.9
9/23/2009	−6.2	−35	16.6
9/30/2009	−5.5		0.8
10/22/2009	−5.4	−25	11.5
11/20/2009	−8.4	−56	11.9
12/31/2009	−5.6		7.9
1/10/2010	−7.3		
1/15/2010	−5.9		
1/15/2010	−7.5		
2/9/2010	−8.0		13.0
2/28/2010	−7.7		3.2
4/5/2010	−4.1		7.1
5/9/2010	−1.9		5.5
6/6/2010	−6.5		7.5
7/1/2010	−7.2	−51	12.5
7/1/2010	−6.8	−41	
8/28/2010	−2.8	−10	8.3
9/7/2010	−8.6	−52	28.9
9/12/2010	−10.5	−74	
10/12/2010	−3.5		3.4
11/9/2010	−2.8		0.7
2/1/2011	−6.0		10.9
4/21/2011	−1.2		2.1
5/13/2011	−2.1		7.6
6/30/2011	−8.0	−59	3.5
12/15/2011	−4.3	−19	7.6
1/30/2012	−4.6	−25	22
3/7/2012	−5.7	−34	11
5/31/2012	−4.4	−28	13.4
9/1/2012	−3.4	−17	7.7
10/9/2012	−6.3	−37	12.1
11/16/2012	−1.6	−2	2.1

^a Sites and methods after Pape et al. (2010).

^b Data from a weather station located in Austin, TX at Camp Mabry (NOAA station ID: TX410428).

4.2. $\delta^{18}\text{O}$ variability

Over the period of April 2009–November 2012, rainfall $\delta^{18}\text{O}$ values ranged from -10.5‰ to 1.0‰ (V-SMOW, Table 3, Fig. 3). There is a weak correlation between monthly rainfall amount and $\delta^{18}\text{O}$ values ($r^2 = 0.34$), whereby $\delta^{18}\text{O}$ values decrease with increasing rainfall amounts at a rate of $\sim 2\text{‰}/100$ mm. There is, however,

no correlation between surface air temperature and rainfall $\delta^{18}\text{O}$. These results are similar to a previous study in central Texas for the period 1999–2007 (Pape et al., 2010).

Drip-water $\delta^{18}\text{O}$ ($\delta^{18}\text{O}_{\text{w}}$) values at the three Westcave drip sites ranged from -4.7‰ to -4.4‰ (mean -4.5‰) over the period of September 2009–March 2011 with no discernible seasonal changes (Fig. 3). Rainfall $\delta^{18}\text{O}$ values thus

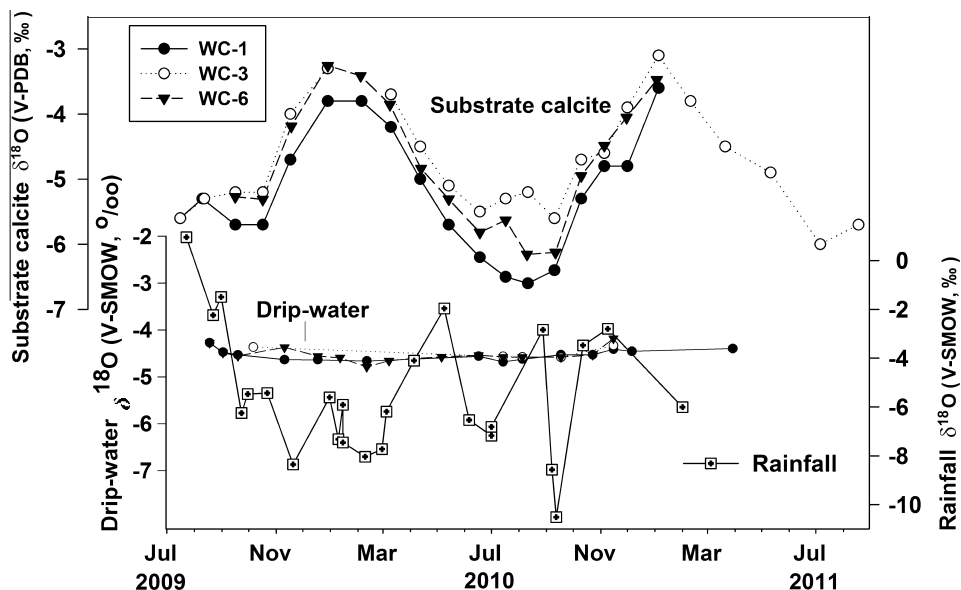


Fig. 3. Time series of $\delta^{18}\text{O}$ values of Austin rainfall, Westcave drip-water and associated substrate calcite samples for each of three drip sites (WC-1, WC-3, and WC-6).

Table 4

The δD and $\delta^{18}\text{O}$ analysis results of Westcave drip-water.

Date of sample collection	$\delta^{18}\text{O}$ (V-SMOW, ‰)	δD (V-SMOW, ‰)
<i>WC-1</i>		
8/4/2011	-4.4	-27
9/1/2011	-4.4	-27
11/13/2011	-4.3	-26
12/15/2011	-4.4	-27
2/6/2012	-4.3	-27
3/8/2012	-4.4	-27
4/12/2012	-4.6	-27
6/2/2012	-4.5	-27
9/21/2012	-4.6	-27
11/2/2012	-4.3	-27
12/19/2012	-4.6	-28
<i>WC-3</i>		
11/13/2011	-4.3	-27
12/15/2011	-4.4	-26
2/6/2012	-4.6	-27
3/8/2012	-4.4	-27
4/12/2012	-4.4	-26
8/4/2011	-4.3	-26
9/21/2012	-4.5	-27
11/2/2012	-4.4	-27
<i>WC-6</i>		
9/1/2011	-4.1	-25
10/6/2011	-4.2	-25
11/13/2011	-4.4	-26
2/6/2012	-4.4	-27
3/8/2012	-4.5	-26
4/12/2012	-4.6	-27
7/19/2012	-4.5	-26
9/21/2012	-4.6	-27
11/2/2012	-4.4	-26

have a 38-fold larger range (11.5‰) than that of the drip-water $\delta^{18}\text{O}_w$ values (0.3‰).

Additional drip-water samples were collected from August 2011 to December 2012 to test the impact of water

Table 5
 r^2 values for linear regressions between substrate calcite $\delta^{18}\text{O}$ values and various temperature measurements.^a

	WC-1	WC-3	WC-6
Average monthly surface air temperature (t_a)	0.95	0.88	0.96
Average monthly cave-air temperature (t_c)	0.84	0.87	0.86
Drip-water temperature (t_w)	0.54	0.67	0.50

^a $p < 0.001$ for all correlations.

evaporation. These samples have $\delta^{18}\text{O}$ values ranging from -4.6‰ to -4.3‰ (WC-1 and WC-3), -4.6‰ to -4.1‰ (WC-6), and δD values from -28‰ to -26‰ (WC-1), -27‰ to -26‰ (WC-3) and -27‰ to -25‰ (WC-6) (Table 4). Drip-water of this period has analytically identical mean $\delta^{18}\text{O}$ values (-4.4‰) as drip-water collected over the study period of 2009–2011.

Substrate calcite samples from three drip sites ($n = 54$, WC-3: July 2009–August 2011; WC-1 and WC-6: Septem-

ber 2009–January 2011) have $\delta^{18}\text{O}$ values ($\delta^{18}\text{O}_{\text{cc}}$) ranging from -6.6‰ to -3.1‰ (V-PDB, Table 2), with all sites showing similar ranges (WC-1: -6.6‰ to -3.6‰ ; WC-3: -6.0‰ to -3.1‰ ; WC-6: -6.2‰ to -3.3‰ ; Fig. 3). The $\delta^{18}\text{O}_{\text{cc}}$ variations are also seasonal, with less negative values in the winters and more negative values in the summers (Fig. 3). The $\delta^{18}\text{O}_{\text{cc}}$ variations do not correlate with amount or $\delta^{18}\text{O}$ values of rainfall, or $\delta^{18}\text{O}_w$ of drip-water, but correlate strongly with temperature (t_a : $r^2 = 0.88\text{--}0.96$,

Table 6
 Oxygen and carbon isotope analysis results for stalagmite WC-3.

Distance from top (mm) ^a	$\delta^{13}\text{C}$ (‰ V-PDB)	$\delta^{18}\text{O}$ (‰ V-PDB)
0.167	-7.7	-4.0
0.334	-8.1	-3.5
0.501	-8.8	-3.1
0.668	-9.1	-3.5
0.835	-9.4	-4.2
1.002	-9.4	-4.9
1.169	-8.9	-4.8
1.336	-8.5	-4.0
1.503	-8.2	-3.1
1.670		
1.837	-8.9	-2.9
2.004	-9.2	-3.3
2.171	-9.3	-4.4
2.338	-8.4	-4.4
2.505	-8.4	-4.4
2.672	-8.7	-4.6
2.839	-8.8	-4.7
3.006	-8.7	-4.6
3.173	-8.4	-4.4
3.340	-8.5	-3.7
3.507	-8.8	-3.2
3.674	-9.0	-3.5
3.841	-9.1	-3.9
4.008		
4.175	-9.2	-4.4
4.342	-8.9	-4.6
4.509	-8.5	-4.6
4.676	-8.7	-4.8
4.843	-8.9	-4.9
5.010	-8.4	-4.8
5.177		
5.344	-7.6	-4.0
5.511	-8.5	-3.9
5.678	-8.9	-3.4
5.845	-9.1	-3.1
6.012	-9.1	-3.6
6.179	-8.4	-4.2
6.346	-8.3	-4.4
6.513	-8.4	-4.7
6.680	-8.6	-4.9

^a Samples were micromilled at 167 μm step.

Table 7
U-series ages for stalagmite WC-3.

Depth (mm)	Age ^a	Age (corrected) ^b	²³⁸ U (ppb)	$\delta^{234}\text{U}_i$	$\delta^{234}\text{U}_p$	²³² Th (pg/g)	²³⁰ Th/ ²³² Th ppm
50	150 ± 9	50 ± 13	572 ± 0.8	182.8 ± 1.3	182.7 ± 1.3	1791 ± 6	9 ± 0.5
65	310 ± 15	160 ± 20	563 ± 1.1	179.7 ± 1.9	179.5 ± 1.9	2532 ± 6	12 ± 0.6
85	150 ± 11	70 ± 13	620 ± 0.8	186.0 ± 1.6	185.9 ± 1.6	1456 ± 7	11 ± 0.8

^a 2-sigma uncertainties.

^b Age corrections were made assuming an initial ²³⁰Th/²³²Th of 5.8 ± 0.6 ppm (Wortham et al., 2013).

$p < 0.001$; t_c : $r^2 = 0.84\text{--}0.87$, $p < 0.001$; and t_w : $r^2 = 0.50\text{--}0.67$, $p < 0.001$; Table 5). Stalagmite WC-3 $\delta^{18}\text{O}$ values (from the upper 6.7 mm of the sample) ranged from -4.9‰ to -2.9‰ (Table 6). There are four cyclical peaks and valleys in the stalagmite $\delta^{18}\text{O}$ time series, with amplitudes of 1.5–2.0‰. On average, each cycle spans a distance of 1.8 mm along the stalagmite's growth axis. Temporal variations of $\delta^{13}\text{C}$ are approximately opposite of $\delta^{18}\text{O}$ values, whereby higher $\delta^{18}\text{O}$ values are mostly associated with lower $\delta^{13}\text{C}$ values. There is, however, no correlation between $\delta^{13}\text{C}$ and $\delta^{18}\text{O}$ values ($r^2 < 0.1$). As $\delta^{13}\text{C}$ values are likely controlled by different factors than those affecting $\delta^{18}\text{O}$ values (Breecker et al., 2012), the $\delta^{13}\text{C}$ results are not discussed further.

From top to bottom, three U-series ages were determined for stalagmite WC-3: 50 ± 13 (at 50 mm), 162 ± 20 (65 mm), 70 ± 13 (85 mm) yrs before present (Table 7). As the middle layer has the oldest age, there is an age reversal. It is possible that the measured modern day ²³⁰Th/²³²Th ratio (Wortham et al., 2013), which was used to calculate corrected ages (Table 7), is different from, or has a larger

uncertainty than, those during deposition of respective dated calcite layers. Nonetheless the measured ratio represents the best value applicable to the specific sample. These three ages correspond to growth rates ranging from 360 to 1500 $\mu\text{m}/\text{yr}$ for WC-3.

5. DISCUSSION

5.1. Reservoir $\delta^{18}\text{O}$ homogenization

For the period of July 2009–February 2011, Austin area rainfall $\delta^{18}\text{O}$ values had a range of 11.5‰, from -10.5‰ to 1‰, with a weighted mean of -6.4‰ (Table 3). This contrasts with the much narrower $\delta^{18}\text{O}_w$ range of 0.3‰ for Westcave drip-waters of the same period (weighted mean: -4.5‰ , Fig. 3). Relatively invariant drip-water $\delta^{18}\text{O}$ values over time are commonly interpreted as an indication of a well-homogenized water reservoir above a cave (e.g., Williams and Fowler, 2002; Pape et al., 2010). Mean rainfall $\delta^{18}\text{O}$ values and mean drip-water $\delta^{18}\text{O}_w$ values are notably different for this study period at Westcave.

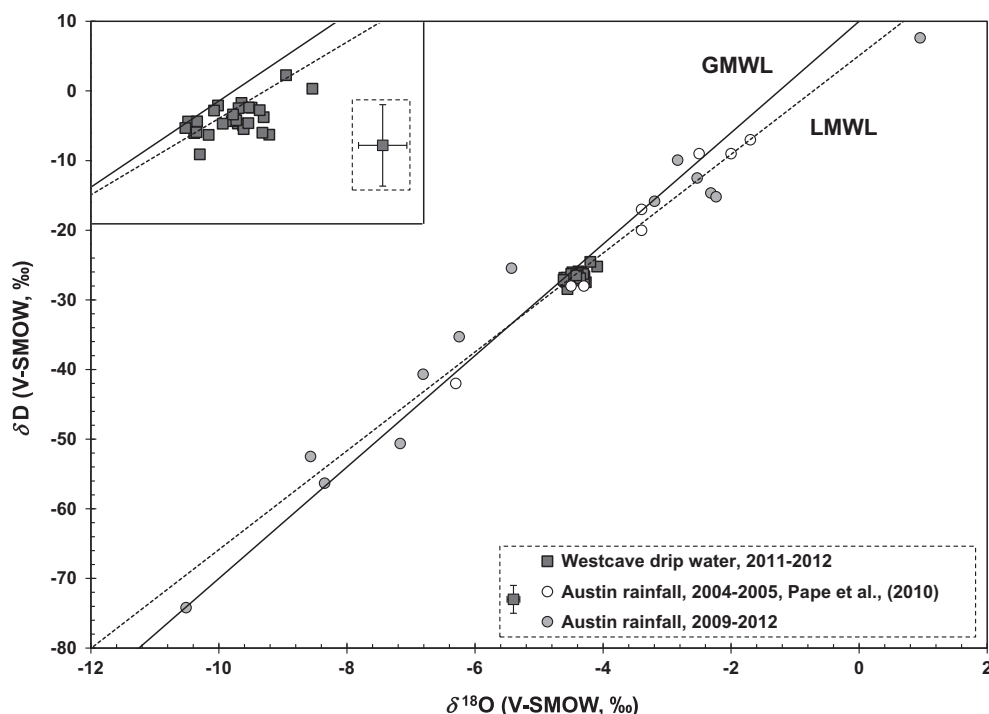


Fig. 4. The δD – $\delta^{18}\text{O}$ variations for Westcave drip-water and Austin rainfall. Rainfall data for 2004–2005 ($n = 8$) are from Pape et al. (2010). Rainfall data for 2009–2011 ($n = 21$) are in Table 3. Data for August 2011–December 2012 Westcave drip-water ($n = 28$) are in Table 4. LMWL is defined by all Austin rainfall data. Within analytical uncertainty, all but six Westcave drip-water samples fall on GMWL, and all but one fall on the LMWL.

Drip-water hydrogen and oxygen isotopic compositions plot along the global and local meteoric water lines (“GMWL” and “LMWL”), indicating that evaporative effects are not significant (Table 4, Fig. 4). The difference between mean rainfall and drip-water $\delta^{18}\text{O}$ values may be a result of (1) geographic differences in rainfall amounts and isotopic compositions between the rainfall collection site (Austin) and the drip-water sites (Westcave); (2) the presence of recharge source(s) other than directly infiltrating rainfall for the vadose reservoir above the cave; or (3) a seasonal bias in recharge feeding drip pathways, wherein a significant fraction of large rainfall events runs-off the surface rather than recharges. In any case, the relatively invariant drip-water $\delta^{18}\text{O}_w$ values imply a well-mixed vadose reservoir and thus provide a framework for interpreting the observed speleothem calcite $\delta^{18}\text{O}$ variations.

5.2. Factors controlling Westcave substrate calcite $\delta^{18}\text{O}$ values

Given a well-mixed vadose water reservoir supplying the drip sites, the variation in speleothem calcite $\delta^{18}\text{O}$ values is likely controlled by one or more of the following in-cave processes: (1) temperature-dependent equilibrium fractionation (e.g., Epstein et al., 1953; Coplen, 2007); (2) kinetic isotope fractionation initiated by rapid CO_2 degassing and calcite deposition (Mickler et al., 2004, 2006; Dreybrodt and Scholz, 2011; Feng et al., 2012); and (3) evaporation (e.g., Hendy, 1971; Deininger et al., 2012). The relative impacts of these factors are discussed below.

5.2.1. Temperature-dependent equilibrium fractionation

Temperature-dependent equilibrium oxygen isotope fractionation between calcite and water, combined with invariant drip-water $\delta^{18}\text{O}$ values, predict that higher temperatures (summer) should be associated with smaller isotopic fractionation and lower $\delta^{18}\text{O}_{\text{cc}}$ values, whereas lower temperatures (winter) should result in larger isotopic fractionation and higher $\delta^{18}\text{O}_{\text{cc}}$ values. These predictions are consistent with the Westcave substrate calcite results (Fig. 3), suggesting a significant control of temperature on these $\delta^{18}\text{O}_{\text{cc}}$ values.

To quantitatively assess the influence of temperature on substrate calcite $\delta^{18}\text{O}_{\text{cc}}$ values, an empirical calcite-water oxygen isotopic fractionation factor can be calculated for each substrate calcite sample using measured drip-water and associated substrate calcite $\delta^{18}\text{O}$ values:

$$\alpha = (\delta_{\text{cc}} + 1) / (\delta_{\text{w}} + 1), \quad (3)$$

δ_{cc} and δ_{w} are the $\delta^{18}\text{O}$ values of calcite and water for the same corresponding time interval, respectively. These calculated α values indicate the extent to which equilibrium fractionation is attained, and the extent of kinetic isotope effects. Calculated α values range from 1.0288 to 1.0324 (Table 2), a variation of 0.0036. Using previously published α – temperature relationships (-0.00017 to -0.0002 /°C, e.g., Epstein et al., 1953; Kim and O’Neil, 1997; Coplen, 2007; Tremaine et al., 2011), this range of α values corresponds to temperature ranges of 18–21 °C. This agrees with the measured range of t_w at all three sites at Westcave. Similar

agreements exist for each of the three individual drip sites. Measured α value ranges are 0.003, 0.0026 and 0.003 for WC-1, WC-3 and WC-6 for substrate samples with both $\delta^{18}\text{O}$ and associated water temperature measurements (Table 2). These values correspond to temperature ranges of 15–18, 13–15 and 15–18 °C, which agree with measured water temperature ranges at the respective sites (13, 15 and 15 °C). These results are consistent with the hypothesis that substrate calcite $\delta^{18}\text{O}_{\text{cc}}$ values are primarily controlled by temperature-dependent equilibrium fractionation.

5.2.2. Kinetic isotope effects

Although temperature-dependent equilibrium fractionation can account for most of the Westcave substrate calcite $\delta^{18}\text{O}_{\text{cc}}$ values, non-equilibrium isotope effects (‘kinetic’ isotope effects) may also influence the $\delta^{18}\text{O}_{\text{cc}}$ values. This is evidenced by the deviation of $\delta^{18}\text{O}_{\text{cc}}$ values from expected equilibrium values based on published equilibrium fractionation factors (Fig. 5a). Whereas there is significant variability in published fractionation factors, the variability in fractionation factors determined using the $\delta^{18}\text{O}_{\text{cc}}$, $\delta^{18}\text{O}_w$, and temperature for the three WC drip sites is not accounted for by any one published factor (Fig. 5a).

Following Feng et al. (2012), the magnitude of a kinetic effect can be calculated as the difference between expected equilibrium calcite $\delta^{18}\text{O}$ ($\delta^{18}\text{O}_e$, calculated using measured water temperature and the fractionation factor of Coplen, 2007) and measured calcite $\delta^{18}\text{O}_{\text{cc}}$:

$$\Delta^{18}\text{O}_{\text{cc-e}} = \delta^{18}\text{O}_{\text{cc}} - \delta^{18}\text{O}_e \quad (4)$$

Non-zero values outside of analytical uncertainty indicate the presence of kinetic effects. These calculated $\Delta^{18}\text{O}_{\text{cc-e}}$ values range from -1.9‰ to 0.7‰ (average -0.6‰ , Table 2). Ninety three percent of the $\Delta^{18}\text{O}_{\text{cc-e}}$ values are negative (64%) or zero (29%). Using the fractionation factor of Tremaine et al. (2011), 61% of the $\Delta^{18}\text{O}_{\text{cc-e}}$ values are negative or zero. There is no significant correlation between drip rates and $\Delta^{18}\text{O}_{\text{cc-e}}$ values for WC-1 and WC-6 substrate calcite. However, a negative correlation exists between drip rate and $\Delta^{18}\text{O}_{\text{cc-e}}$ at WC-3 ($r^2 = 0.43$), whereby faster drip rate led to more negative $\Delta^{18}\text{O}_{\text{cc-e}}$ values. These negative $\Delta^{18}\text{O}_{\text{cc-e}}$ values are consistent with the hypothesis that calcite deposits by surface trapping of CO_3^{2-} with more negative $\delta^{18}\text{O}$ values than those in the calcite’s inner lattice (e.g., Watson, 2004; Feng et al., 2012). Faster calcite deposition rate removes the calcite surface layer more quickly from isotopic exchange with water, thus hindering ion diffusion and preventing isotopic equilibrium from being achieved. This hypothesis implies that a faster calcite deposition rate leads to more negative calcite $\delta^{18}\text{O}$ values.

This hypothetical relationship between $\Delta^{18}\text{O}_{\text{cc-e}}$ and calcite growth rate is observed for WC-1 substrate calcites, whereby $\Delta^{18}\text{O}_{\text{cc-e}}$ values vary seasonally. Near-zero values were observed for calcite deposited in the winter months and more negative values in the summer months at this site. Linear regression between $\Delta^{18}\text{O}_{\text{cc-e}}$ and substrate calcite growth rate yields a weak, but notable correlation (Fig. 5b; $r^2 = 0.29$, $p < 0.05$, $n = 14$). A similar correlation is not observed in WC-3 ($r^2 \leq 0.05$) or WC-6 ($r^2 = 0.12$) samples. For WC-3, the site of our stalagmite sample, $\Delta^{18}\text{O}_{\text{cc-e}}$ values

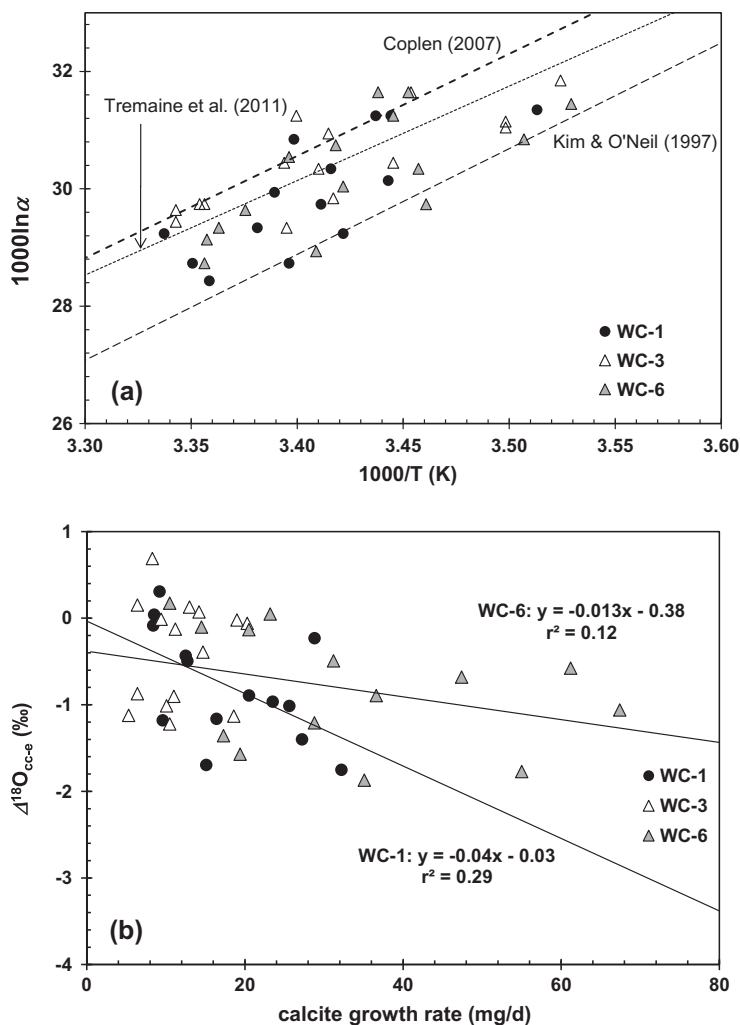


Fig. 5. Comparison of measured substrate calcite $\delta^{18}O$ values with predicted equilibrium values. (a) Measured calcite-water oxygen isotope fractionation vs. drip-water temperature ($1000\ln\alpha$ vs. $1000/T$). Lines depicting equilibrium calcite-water fractionations are based on equations from published studies in laboratory and natural systems (Kim and O'Neil, 1997; Coplen, 2007; Tremaine et al., 2011). WC drip sites results were determined using measured $\delta^{18}O_{cc}$, $\delta^{18}O_w$, and water temperature. (b) $\Delta^{18}O_{cc-e}$ (measured $\delta^{18}O_{cc}$ minus equilibrium $\delta^{18}O_e$) compared with calcite growth rates.

range from -1.2‰ to 0.7‰ , and 53% of the $|\Delta^{18}O_{cc-e}|$ values are 0.4‰ or less. This smaller $\Delta^{18}O_{cc-e}$ range (than the other two sites), and lack of seasonal variation of $\Delta^{18}O_{cc-e}$ values of WC-3 substrate calcite indicate that kinetic effects are not a significant control on calcite $\delta^{18}O_{cc}$ values for most of the WC-3 substrate samples.

Enhanced evaporation of the water film on the surface of a speleothem could lead to more positive $\delta^{18}O$ values in the residual water and resulting calcite (Hendy, 1971; Deininger et al., 2012). The majority of calculated speleothem calcite $\Delta^{18}O_{cc-e}$ values are negative, however, indicating more negative $\delta^{18}O$ values in speleothem calcite compared to the predicted equilibrium values. This suggests that evaporative effects are not a dominant factor influencing the $\delta^{18}O$ of substrate calcite. This is consistent with the inference of lack of evaporation in drip water before dripping, evidenced by hydrogen and oxygen isotopic compositions plotting along the GMWL and LMWL (Fig. 4).

5.3. Empirical $\delta^{18}O_{cc}$ – temperature relationship

Although ambient cave temperature appears to be the dominant control on Westcave substrate calcite $\delta^{18}O$ values, temperature-dependent equilibrium fractionation factors pertain to the relationship between calcite $\delta^{18}O_{cc}$, drip-water $\delta^{18}O_w$, and water temperature (t_w). An empirical correlation between surface air temperature (t_a) and substrate calcite $\delta^{18}O$ is potentially more useful because surface air temperature is of direct interest to climate researchers. The discrepancy between the temperature records is due to: (1) the surface air temperature was measured daily whereas the in-cave measurements are spot measurements taken periodically; and (2) the cave-air temperature and water temperature are affected by vegetation shading and regulation of a body of water nearby. The continuity of the surface air temperature record also most closely corresponds to the continuous growth of calcite on the substrates and the stalagmite.

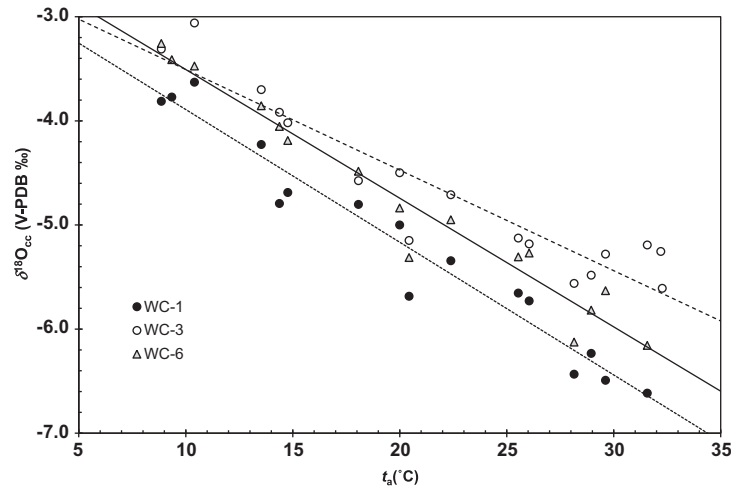


Fig. 6. Substrate calcite $\delta^{18}\text{O}$ values vs. instrumented surface air temperature (t_a). Strong linear correlations exist for all three monitored drip sites (dotted line: WC-1; dash line: WC-3; solid line: WC-6), whereas there are slight differences in slope and intercept of the regression for each drip site (Eqs. (5a), (5b), (5c)). Linear regression for site WC-3 yields Eq. (5b) (see text), which is used to derive a past temperature record from stalagmite WC-3 growing at this drip site.

An empirical correlation between t_a and substrate calcite $\delta^{18}\text{O}$ values should include the effects of not only equilibrium and kinetic fractionation processes, but also factors that control differences in t_w and t_a . Because each drip site has slight differences between drip-water temperature and cave-air temperature (even though they are affected by the same surface air temperature) and drip characteristics (i.e., drip rate), a linear regression between t_a and $\delta^{18}\text{O}$ is constructed for each of the three drip sites (Fig. 6):

$$\text{For site WC-1: } t_a = -7.5(\pm 0.4) \times \delta^{18}\text{O} \times 10^3 - 19.6(\pm 2.3); r^2 = 0.95 \quad (5a)$$

$$\text{For site WC-3: } t_a = -9.1(\pm 0.9) \times \delta^{18}\text{O} \times 10^3 - 20.6(\pm 4.1); r^2 = 0.88 \quad (5b)$$

$$\text{For site WC-6: } t_a = -7.7(\pm 0.4) \times \delta^{18}\text{O} \times 10^3 - 16.7(\pm 2.1); r^2 = 0.96 \quad (5c)$$

These relationships yield uncertainties on temperature estimates of 4, 9 and 4 °C for Eqs. (5a), (5b), (5c), respectively, for a typical $\delta^{18}\text{O}$ value of -4‰ . Although these uncertainties on absolute temperature estimates are significant, these relationships may be used to reconstruct variations in past surface temperatures based on $\delta^{18}\text{O}$ values of stalagmites collected from these drip sites, as discussed below.

5.3.1. Absolute temperature reconstruction

The apparent primary control of ambient cave temperature on calcite $\delta^{18}\text{O}$ values at Westcave suggests that paleotemperature records may be reconstructed from stalagmite $\delta^{18}\text{O}$ values. We test this by applying the empirical surface air temperature– $\delta^{18}\text{O}$ relationship from substrate calcite (Eq. (5b), for site WC-3) to reconstruct a temperature record using $\delta^{18}\text{O}$ values measured on samples collected continuously over the upper 6.7 mm of stalagmite WC-3 (Fig. 1c).

For the four cycles that constitute the stalagmite WC-3 $\delta^{18}\text{O}$ time series (Fig. 7), the magnitude of peak-to-valley

shifts are 1.5–2.0‰. If temperature were the only control on these $\delta^{18}\text{O}$ values, these shifts would correspond to a temperature variation of 14–18 °C (Eq. (5b)). This variation is similar to the recorded seasonal temperature change in the region (19–23 °C). The peaks likely record winter calcite deposition at slower rates, whereas valleys represent summer calcite deposition at faster rates. These inferences indicate that the upper 6.7 mm of stalagmite WC-3 represents the period from the summer of 2005 to the summer of 2009. This interpretation of seasonal cycles is supported by several lines of evidence. First, the higher density of samples from valleys compare to peaks due to constant-interval (167 μm) sampling (Fig. 7) suggests faster calcite deposition during warm seasons (when calcite $\delta^{18}\text{O}$ is low). Secondly, the range of stalagmite $\delta^{18}\text{O}$ values (-4.9‰ to -2.9‰) is similar to that of substrate calcite $\delta^{18}\text{O}_{\text{cc}}$ values (-6.0‰ to -3.1‰). The variations in calcite $\delta^{18}\text{O}$ values also agree with seasonal Sr/Ca, Ba/Ca, and Mg/Ca variations in WC-3 drip-water, WC-3 substrate calcite and stalagmite WC-3 (Casteel and Banner, 2011; Miller et al., 2012). Finally, U-series geochronology permits interpretation of $\delta^{18}\text{O}$ peaks and valleys as seasonal variations. The three U-series ages result in stalagmite growth rates of 360–1,500 $\mu\text{m}/\text{yr}$. This indicates that the sample collection interval (167 $\mu\text{m}/\text{sample}$) represents 1/10 to 1/2 of annual sample growth, and therefore is small enough to resolve seasonal changes.

The stalagmite-derived 2005–2009 surface air temperature record shows a 0–8 °C offset towards cooler temperatures from the weather station record (Fig. 8). The offset between the two records is smaller during low temperature months than high temperature ones. This is likely a result of slower speleothem growth in winter months than in summer months. Given our equal-distance sampling, the low temperature intervals in the speleothem record represent multiple months of calcite deposition, recording a temperature warmer than the lowest single monthly temperature in the instrumental record. This offset is unlikely to be caused by kinetic effects observed in substrate calcite, as its effect

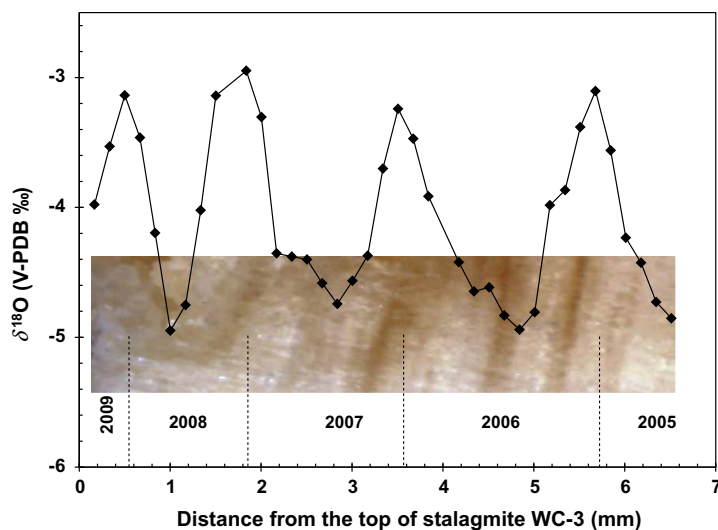


Fig. 7. The $\delta^{18}\text{O}$ values for the top 6.7 mm of stalagmite WC-3. Samples were collected along a transect parallel to the growth axis at an interval of 167 μm . The $\delta^{18}\text{O}$ values are plotted against distance from top surface of the sample. The cyclic $\delta^{18}\text{O}$ variations are likely seasonal (see text). The record ends in the summer of 2009, when the stalagmite was sampled. Each year starts and ends at two adjacent peak $\delta^{18}\text{O}$ values, inferred to represent coolest temperatures of the year (i.e., January and December). Superimposed is a scanned image of the top of the stalagmite.

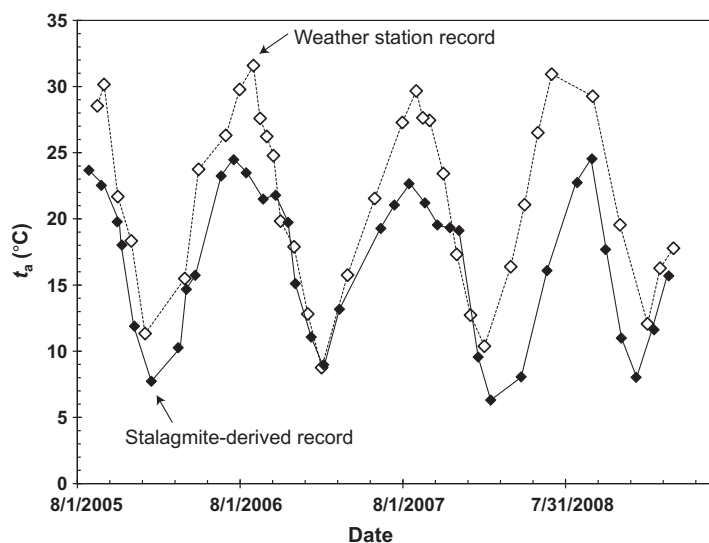


Fig. 8. Comparison of time series of monthly average instrumented temperature from 2005 to 2009 from nearby weather station (open symbols) with the stalagmite WC-3 $\delta^{18}\text{O}$ -derived temperature record using Eq. (5b) (filled symbols). The inferred ages for stalagmite WC-3 samples are adjusted to match the peaks and valleys of weather station temperature record.

is incorporated into Eq. (5b). The extents of kinetic effect, however, may be different for the period of 2005–2009. The offset between two records could also be due to one or more of the following factors. First, it may be a result of the large uncertainty (9 °C when $\delta^{18}\text{O}_{\text{cc}} = -4\text{‰}$) associated with Eq. (5b). Second, drip-water $\delta^{18}\text{O}$ during 2005–2009 may have been 1–2‰ higher compared to 2009–2011, for which the measured drip-water $\delta^{18}\text{O}$ value of -4.5‰ was required to derive Eq. (5b). Westcave annual rainfall averaged ~ 66 cm for 2005–2009 and 91 cm for 2009–2011. The increased amount during 2009–2011 could have produced rainfall with decreased $\delta^{18}\text{O}$ values (Pape

et al., 2010). Even though Westcave drip-waters were well homogenized in terms of $\delta^{18}\text{O}$ values during the study period, drip-water was not collected during the period 2005–2009 and may have been more positive than those from 2009 to 2011. Uncertainties of temperature reconstruction may also result from (1) the differences in growth mechanism (and, therefore, non-equilibrium effects) between the flat substrate morphology and the curved stalagmite surface, and (2) the porous nature of the stalagmite growth axis that represents periodic depressions in the growth surface. These depressions may prolong drip-water residence time and engender evaporation on the stalagmite surface.

With a longer stalagmite record and substrate record, a statistically more robust calibration could be made for reconstructing temperature records from speleothem $\delta^{18}\text{O}$ values.

5.3.2. Intra- and inter-annual temperature variations

Despite the offset between the speleothem $\delta^{18}\text{O}$ derived temperature record and the instrumental record, the derived temperature record implies seasonal temperature changes of 14–18 °C for the 2005–2009 time period. These temperature predictions are similar to the instrumental seasonal temperature range of 19–23 °C for the same period,

particularly when considering the large uncertainties associated with Eq. (5b). As seasonality is an important meteorological parameter that has a significant impact on various chemical, geological, and biological processes (e.g., Mysterud et al., 2011; Yang et al., 2012), speleothem-derived temperature records from settings like Westcave may provide valuable insight into temporal changes in seasonality.

Speleothem-derived temperature records may also provide information on changes in inter-annual summer peak temperatures. Combining substrate calcite (Table 2) and stalagmite WC-3 records (Table 6), a seven year $\delta^{18}\text{O}$

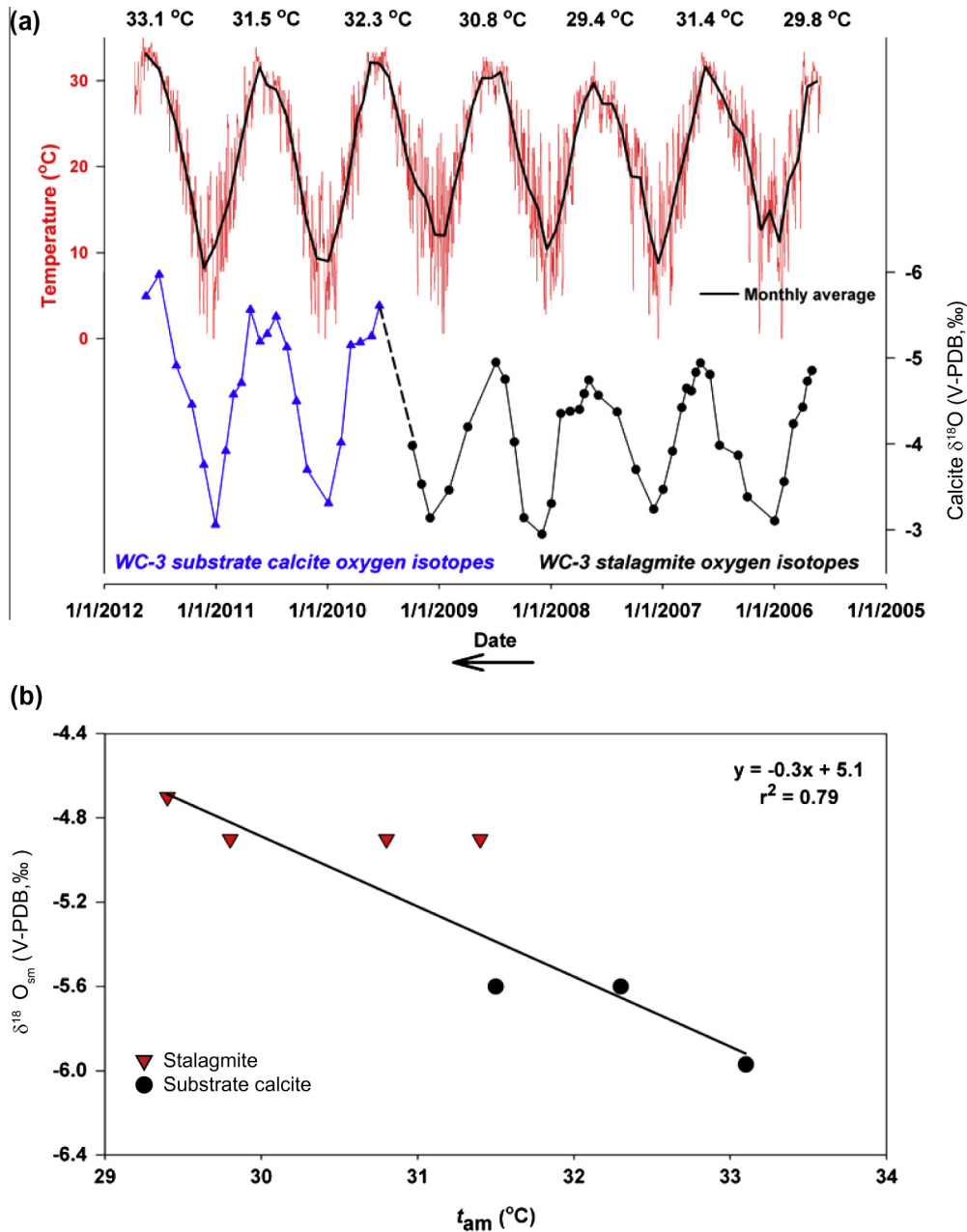


Fig. 9. (a) Comparison of time series of daily (red) and monthly mean (black) instrumented temperature and WC-3 substrate and stalagmite calcite $\delta^{18}\text{O}$. Ages for substrate calcite are midpoint of time interval of substrate deployment; ages for stalagmite WC-3 samples are adjusted to match the peaks and valleys of the temperature record. (b) Linear regression between summer peak temperatures and corresponding calcite $\delta^{18}\text{O}$ values. (For interpretation of the references to colour in this figure legend, the reader is referred to the web version of this article.)

record can be constructed (Fig. 9a). The most negative $\delta^{18}\text{O}$ values in each cycle correspond to calcite deposited in the warmest months of the year. The six seasonal minimum $\delta^{18}\text{O}$ values ($\delta^{18}\text{O}_{\text{sm}}$) correlate with the recorded maximum mean monthly surface air temperature (t_{am}) (Fig. 9b). Linear regression yields:

$$\delta^{18}\text{O}_{\text{sm}} = -0.3(\pm 0.1) \times t_{\text{am}} + 5.1(\pm 2.4) \quad r^2 = 0.79 \quad (6)$$

The slightly higher value for this slope (-0.3) than predicted by equilibrium fractionation factors may be due to kinetic effects in fast-growing calcite. Still, this slope is identical (within uncertainty) to the $\sim -0.2\text{‰}/^\circ\text{C}$ proposed for the temperature-dependent equilibrium fractionation between calcite and water in published studies (e.g., Epstein et al., 1953; Kim and O'Neil, 1997; Coplen, 2007). This is consistent with temperature variation as the main control governing Eq. (6), and that drip-water $\delta^{18}\text{O}$ did not change significantly during this period. Therefore, Eq. (6) may be used to infer relative changes in intra-annual summer peak temperatures using the stalagmite WC-3. Note that a similar relationship between winter minimum temperature and $\delta^{18}\text{O}$ values cannot be obtained from this data set due to slower growth of calcite in the winter months and overall small $\delta^{18}\text{O}$ range ($<0.4\text{‰}$) of calcite deposited during the winter months.

5.4. Implications for paleoclimate studies

The seasonal temperature cycles recorded in Westcave speleothems, as reflected in $\delta^{18}\text{O}$ values, may also serve as a chronometer that can provide sub-annual age constraints. Results from this study further indicate that quantitative inter- and intra-annual variations in surface air temperature can be inferred from speleothem $\delta^{18}\text{O}$ when certain conditions are met.

The first condition is invariable or known drip-water $\delta^{18}\text{O}$ values. Although high-resolution drip-water $\delta^{18}\text{O}$ records may be difficult to infer for speleothem calcite deposited in the past, low-resolution records can be acquired by analyzing speleothem fluid inclusions (e.g., Vonhof et al., 2006). These low-resolution drip-water $\delta^{18}\text{O}$ records may be helpful when an assumption of invariable drip-water $\delta^{18}\text{O}$ values is valid for multiple years. Such assumptions can be tested through modern monitoring studies (e.g., Pape et al., 2010). The second requirement for using speleothem $\delta^{18}\text{O}$ to infer seasonal temperatures is that the speleothem growth must be fast enough to permit sub-annual sampling for $\delta^{18}\text{O}$ analysis. Even if samples grew too slowly for sub-annual sampling using micromilling, this condition may be met by methods such as secondary ion mass spectrometry, which is capable of sampling resolution on the order of $10\mu\text{m}$, but at a lower precision than traditional isotope ratio mass spectrometer (e.g., Orland et al., 2009). Lastly, significant temperature variations are needed in the speleothem growth environment. Westcave provides such an environment, yet most caves in speleothem studies are much deeper and have little to no change in seasonal temperatures (e.g., Feng et al., 2012). This raises the question: How applicable is the approach outlined in the present study? We note that the portions of caves near their entrances can maintain low,

atmospheric-level CO_2 concentrations and experience significant seasonal changes in temperature, not unlike Westcave. These portions of caves have typically been under-studied because deeper portions of caves are preferred in paleoclimate research due to a more stable depositional environment for calcite. Factors that may complicate the interpretation of $\delta^{18}\text{O}$ records from near-entrance speleothems include high rates of evaporation and CO_2 degassing from drip-waters, both of which may engender kinetic isotope fractionation (Hendy, 1971; Mickler et al., 2004, 2006; Dreybrodt and Scholz, 2011; Feng et al., 2012). Therefore, although oxygen isotope analysis of speleothems from shallow portions of caves may have potential as a paleotemperature proxy, monitoring of the modern environment will be essential to assess the variations (or lack thereof) in drip-water $\delta^{18}\text{O}$ values and relationship between speleothem $\delta^{18}\text{O}$ value and ambient temperature.

6. CONCLUSIONS

Analysis of $\delta^{18}\text{O}$ variations of rainfall, drip-water, modern substrate calcite, and a stalagmite from Westcave in central Texas provides insights on the prospects for using speleothem $\delta^{18}\text{O}$ values for the reconstruction of past temperatures and allow us to reach the following conclusions.

- (1) Drip-waters at all three Westcave sites studied had relatively invariable $\delta^{18}\text{O}$ values over a multi-year monitoring period, indicating that drip sites are fed by a well-homogenized vadose reservoir.
- (2) The $\delta^{18}\text{O}$ values of substrate calcite deposited in the cave vary seasonally and have a strong linear relationship with surface air, cave-air, and drip-water temperatures. The control on $\delta^{18}\text{O}$ values is primarily temperature-dependent equilibrium fractionation and, to a lesser extent, kinetic fractionation processes.
- (3) Applying an empirical relationship between surface air temperature and substrate calcite $\delta^{18}\text{O}$ from a monitored drip site to a stalagmite $\delta^{18}\text{O}$ time series yields a seasonal temperature record. The speleothem derived record displays an offset towards lower temperatures when compared to the instrumental record, but show comparable amplitudes of seasonal ranges ($14\text{--}18^\circ\text{C}$ vs. $19\text{--}23^\circ\text{C}$) and inter-annual variations for summer peak temperatures.
- (4) With constant or known drip-water $\delta^{18}\text{O}$ values, records of absolute temperature, seasonality, and relative peak summer temperature changes may be derived from $\delta^{18}\text{O}$ time series of speleothems growing near cave entrances. Interpretation of such records requires high-resolution (monthly) and long term (>1 yr) monitoring studies of specific drip sites under which speleothems grow to calibrate relationships between temperature and calcite $\delta^{18}\text{O}$ values.

ACKNOWLEDGEMENTS

This research was supported by NSF P2C2 grant ATM-0823665, NSF REU grants EAR-0852029 and EAR-1157031,

NSF Geobiology and Low Temperature Geochemistry grant EAR-1124514 and by the Geology Foundation and Environmental Science Institute of the University of Texas. Comments from three anonymous reviewers and discussions with Nate Miller, Dan Breecer and Eric James improved the manuscript. We wish to thank John Ahrns and the management and staff at Westcave Preserve, and many others over the past decade for assistance in the field.

REFERENCES

- Asmerom Y. et al. (2010) Variable winter moisture in the southwestern United States linked to rapid glacial climate shifts. *Nat. Geosci.* **3**, 114–117.
- Affek H., Bar-Matthews M., Ayalon A., Matthews A. and Eiler J. (2008) Glacial/interglacial temperature variations in Soreq cave speleothems as recorded by ‘clumped isotope’ thermometry. *Geochim. Cosmochim. Acta* **72**, 5351–5360.
- Banner J. L., Guilfoyle A., James E. W., Stern L. A. and Musgrove M. (2007) Seasonal variations in modern speleothem calcite growth in central Texas, USA. *J. Sediment. Res.* **77**, 615–622.
- Banner J. L., Jackson C. S., Zong-Liang Y., Hayhoe K., Woodhouse C., Gulden L., Jacobs K., North G., Washington R., Jiang X. and Casteel R. (2010) Climate change impacts on Texas water: A white paper assessment of the past, present and future and recommendations for action. *Texas Water Journal* **1**, 1.
- Bar-Matthews M., Ayalon A., Kaufman A. and Wasserburg G. J. (1999) The Eastern Mediterranean paleoclimate as a reflection of regional events: Soreq cave, Israel. *Earth Planet. Sci. Lett.* **166**, 85–95.
- Breecker D. O., Payne A. E., Quade J., Banner J. L., Ball C. E., Meyer K. W. and Cowan B. D. (2012) The sources and sinks of CO₂ in caves under mixed woodland and grassland vegetation. *Geochimica et Cosmochimica Acta* **96**, 230–246.
- Casteel R. C. (2011) The modern assessment of climate, calcite growth, and the geochemistry of cave drip-waters as a precursor to paleoclimate study. M.S. thesis, University of Texas, Austin. <http://hdl.handle.net/2152/ETD-UT-2011-08-4177>.
- Casteel R. C. and Banner J. L. (2011) Speleothem calcite deposition rates and cave drip water trace element variations as a function of seasonal temperature variability in central Texas, USA. Abstract PP31C-1874 presented at 2011 Fall Meeting, AGU, San Francisco, Calif., 5–9 Dec.
- Cheng H. et al. (2000) The half-lives of uranium-234 and thorium-230. *Chem. Geol.* **169**, 17–33.
- Cheng H. et al. (2009) Ice age terminations. *Science* **326**, 248–252.
- Combs S. (2012) The impact of the 2011 drought and beyond. State of Texas Report 96–1704. Austin, TX. <http://www.window.state.tx.us/specialrpt/drought/pdf/96-1704-Drought.pdf>.
- Coplen T. B. (1996) New guidelines for reporting stable hydrogen, carbon, and oxygen isotope-ratio data. *Geochim. Cosmochim. Acta* **60**, 3359–3360.
- Coplen T. B. (2007) Calibration of the calcite-water oxygen-isotope geothermometer at Devils Hole, Nevada, a natural laboratory. *Geochim. Cosmochim. Acta* **71**, 3948–3957.
- Cowan B., Osborne M. and Banner J. L. (2013) Temporal variability of cave-air CO₂ in central Texas. *J. Cave Karst Studies* **75**, 38–50.
- Craig H. (1957) Isotopic standards for carbon and oxygen and correction factors for mass spectrometric analysis. *Geochim. Cosmochim. Acta* **12**, 133–144.
- Daëron M., Guo W., Eiler J., Genty D., Blamart D., Boch R., Drysdale R., Maire R., Wainer K. and Zanchetta G. (2011) ¹³C/¹⁸O clumping in speleothems: observations from natural caves and precipitation experiments. *Geochim. Cosmochim. Acta* **75**, 3303–3317.
- Deininger M., Fohlmeister J., Scholz D. and Mangini A. (2012) Isotope disequilibrium effects: The influence of evaporation and ventilation effects on the carbon and oxygen isotope composition of speleothems – a model approach. *Geochim. Cosmochim. Acta* **96**, 57–79.
- Dreybrodt W. and Scholz D. (2011) Climatic dependence of stable carbon and oxygen isotope signals recorded in speleothems: from soil water to speleothem calcite. *Geochim. Cosmochim. Acta* **75**, 734–752.
- Epstein S., Buchsbaum R., Lowenstam H. and Urey H. C. (1953) Revised carbonate-water isotopic temperature scale. *Bull. Geol. Soc. Am.* **64**, 1315–1326.
- Feng W., Banner J., Guilfoyle A., Musgrove M. and James E. W. (2012) Oxygen isotopic fractionation between drip water and speleothem calcite: A 10-year monitoring study, central Texas, USA. *Chem. Geol.* **304–305**, 53–67.
- Frappier A. B., Sahagian D., Carpenter S. J., González L. A. and Frappier B. R. (2007) A stalagmite proxy record of recent tropical cyclone events. *Geology* **7**, 111–114.
- Friedman I. and O’Neil J. R. (1977) Compilation of isotopic fractionation factors of geochemical interest. US Geological Survey Professional Paper. 440-KK.
- Gonfiantini R. (1978) Standards for stable isotope measurements in natural compounds. *Nature* **271**, 534–536.
- Hendy C. H. (1971) The isotopic geochemistry of speleothems-I. The calculation of the effects of different modes of formation on the isotopic composition of speleothems and their applicability as palaeoclimatic indicators. *Geochim. Cosmochim. Acta* **35**, 801–824.
- Hu C., Henderson G. M., Huang J., Xie S., Sun Y. and Johnson K. R. (2008) Quantification of Holocene Asian monsoon precipitation from spatially separated cave records. *Earth Planet. Sci. Lett.* **266**, 221–232.
- Johnson K. R., Hu H., Belshaw N. S. and Henderson G. M. (2006) Seasonal trace element and stable isotope variations in a Chinese speleothem: the potential for high-resolution paleomonsoon reconstruction. *Earth Planet. Sci. Lett.* **244**, 394–407.
- Kim S. and O’Neil J. R. (1997) Equilibrium and nonequilibrium oxygen isotope effects in synthetic carbonates. *Geochim. Cosmochim. Acta* **61**, 3461–3475.
- Lachniet M. S., Burns S. J., Piperno D. R., Asmerom Y., Polyak V. J., Moy C. M. and Christenson K. (2004) A 1500 year El Niño/Southern oscillation and rainfall history for the Isthmus of Panama from speleothem calcite. *J. Geophys. Res. D Atmos.* **109**. <http://dx.doi.org/10.1029/2004JD004694>.
- Larkin T. J. and Bomar G. W. (1983) Climatic atlas of Texas: Texas Water Development Board Limited Publication **192**, 151 pp. http://www.twdb.state.tx.us/publications/reports/limited_printing/doc/LP192.pdf.
- Mattey D., Lowry W., Duffet J., Fisher R., Hodge E. and Frisia S. (2008) A 53 year seasonally resolved oxygen and carbon isotope record from a modern Gibraltar speleothem: reconstructed drip water and relationship to local precipitation. *Earth Planet. Sci. Lett.* **269**, 80–95.
- Mickler P. J., Banner J. L., Stern L. A., Asmerom Y., Edwards R. L. and Ito E. (2004) Stable isotope variations in modern tropical speleothems: evaluating equilibrium vs. kinetic isotope effects. *Geochim. Cosmochim. Acta* **68**, 4381–4393.
- Mickler P. J., Stern L. A. and Banner J. L. (2006) Large kinetic isotope effects in modern speleothems. *GSA Bull.* **118**, 65–81.
- Miller N. R., Griffiths R. E. and Banner J. (2012) It’s okay. We’re in the band – importance of oriented band fabric imagery for establishing high-resolution trace element time-series in

- slow-growth speleothems by LA-ICP-MS. *Geol. Soc. Am. Abstracts with Programs* **44**, 585.
- Musgrove M., Banner J. L., Mack L. E., Combs D. M., James E. W., Cheng H. and Edwards R. L. (2001) Geochronology of late Pleistocene to Holocene speleothems from central Texas: implications for regional paleoclimate. *GSA Bull.* **113**, 1532–1543.
- Musgrove M. and Banner J. L. (2004) Controls on the spatial and temporal variability of vadose dripwater geochemistry: Edwards Aquifer, central Texas. *Geochim. Cosmochim. Acta* **68**, 1007–1020.
- Mysterud A., Hessen D. O., Moberg R., Martinsen V., Mulder J. and Austrheim G. (2011) Plant quality, seasonality and sheep grazing in an alpine ecosystem. *Basic Appl. Ecol.* **12**, 195–206.
- Orland I., Barmathews M., Kita N., Ayalon A., Matthews A. and Valley J. (2009) Climate deterioration in the Eastern Mediterranean as revealed by ion microprobe analysis of a speleothem that grew from 2.2 to 0.9 ka in Soreq Cave, Israel. *Quater. Res.* **71**, 27–35.
- Pape J. R., Banner J. L., Mack L. E., Musgrove M. and Guilfoyle A. (2010) Controls on oxygen isotope variability in precipitation and cave drip-waters, central Texas, USA. *J. Hydrol.* **385**, 203–215.
- Kluge T., Marx T., Scholz D., Niggemann S., Mangini A. and Aeschbach-Hertig W. (2008) A new tool for palaeoclimate reconstruction: Noble gas temperatures from fluid inclusions in speleothems. *Earth Planet. Sci. Lett.* **269**, 407–414.
- Scheidegger Y., Baur H., Brennwald M. S., Fleitmann D., Wieler R. and Kipfer R. (2010) Accurate analysis of noble gas concentrations in small water samples and its application to fluid inclusions in stalagmites. *Chem. Geol.* **272**, 31–39.
- Scholz D., Mühlinghaus C. and Mangini A. (2009) Modelling $\delta^{13}\text{C}$ and $\delta^{18}\text{O}$ in the solution layer on stalagmite surfaces. *Geochim. Cosmochim. Acta.* **73**, 2592–2602.
- Shakun J. D., Burns S. J., Fleitmann D., Kramers J., Matter A. and Al-Subary A. (2007) A high-resolution, absolute-dated deglacial speleothem record of Indian Ocean climate from Socotra Island, Yemen. *Earth Planet. Sci. Lett.* **259**, 442–456.
- Rozanski K., Araguas-Araguas L. and Gonfiantini R. (1993) Isotopic patterns in modern global precipitation. *AGU Geophys. Monogr.* **78**, 1–36.
- Tremaine D. M., Froelich P. N. and Wang Y. (2011) Speleothem calcite formed in situ: Modern calibration of $\delta^{18}\text{O}$ and $\delta^{13}\text{C}$ paleoclimate proxies in a continuously monitored natural cave system. *Geochim. Cosmochim. Acta* **75**, 4929–4950.
- Vonhof H. B., van Breukelen M. R., Postma O., Rowe P. J., Atkinson T. C. and Kroon D. (2006) A continuous-flow crushing device for on-line $\delta^2\text{H}$ analysis of fluid inclusion water in speleothems. *Rapid Commun. Mass Spectrom.* **20**, 2553–2558.
- Wagner J. D. M., Cole J. E., Beck J. W., Patchett P. J., Henderson G. M. and Barnett H. R. (2010) Moisture variability in the southwestern United States linked to abrupt glacial climate change. *Nat. Geosci.* **3**, 110–113.
- Wang Y. J., Cheng H., Edwards R. L., An Z. S., Wu J. Y., Shen C. C. and Dorale J. A. (2001) A high-resolution absolute-dated Late Pleistocene monsoon record from Hulu Cave, China. *Science* **294**, 2345–2348.
- Watson E. B. (2004) A conceptual model for near-surface kinetic controls on the trace-element and stable isotope composition of abiogenic calcite crystals. *Geochim. Cosmochim. Acta* **68**, 1473–1488.
- Williams R. W. and Fowler A. (2002) Relationship between oxygen isotopes in rainfall, cave percolation waters and speleothem calcite at Waitomo, New Zealand. *J. Hydrol.* **41**, 53–70.
- Wortham B., James E.W. and Banner J.L. (2013) Variability in initial $^{230}\text{Th}/^{232}\text{Th}$ ratios in central Texas speleothems is used for more accurate age determination. *Geol. Soc. Am. South-Central Section – 47th Annual Meeting, Abstract*, 17.
- Yang S., Ding Z., Wang X., Tang Z. and Gu Z. (2012) Negative $\delta^{18}\text{O}$ – $\delta^{13}\text{C}$ relationship of pedogenic carbonate from northern China indicates a strong response of C3/C4 biomass to the seasonality of Asian monsoon precipitation. *Palaeogeogr. Palaeoclimatol. Palaeoecol.* **317–318**, 32–40.

Associate editor: Marc Norman